Kinetics of the Reduction of Dialkyl Peroxides. New Insights into the Dynamics of Dissociative Electron Transfer[1]

Robert L. Donkers,[†] Flavio Maran,*[,‡] Danial D. M. Wayner,*[,§] and Mark S. Workentin*[,†]

Contribution from the Department of Chemistry, The University of Western Ontario, London, ON Canada N6A 5B7, Dipartimento di Chimica Fisica, Università di Padova, Via Loredan 2, 35131 Padova, Italy, and Steacie Institute for Molecular Sciences, National Research Council of Canada, Ottawa, ON Canada K1A 0R6

Received February 26, 1999

Abstract: The concerted dissociative reduction of di-*tert*-butyl peroxide (DTBP), dicumyl peroxide (DCP), and di-*n*-butyl peroxide (DNBP) is evaluated by both heterogeneous and homogeneous electron transfer using electrochemical methods. Electrochemical and thermochemical determination of the O−O bond energies and the standard potentials of the alkoxyl radicals allow the standard potentials for dissociative reduction of the three peroxides in *N*,*N*-dimethylformamide and acetonitrile to be evaluated. These values allowed the kinetics of homogeneous ET reduction of DTBP and DCP by a variety of radical anion donors to be evaluated as a function of overall driving force. Comparison of the heterogeneous ET kinetics of DTBP and DNBP as a function of driving force for ET allowed the distance dependence on the reduction kinetics of the former to be estimated. Results indicate that the kinetics of ET to DTBP is some 0.8 order of magnitude slower in reactivity than DNBP because of a steric effect imposed by the bulky *tert*-butyl groups. Experimental activation parameters were measured for the homogeneous reduction of DTBP with five mediators, covering a range of 0.4 eV in driving force over the temperature range −30 to 50 °C in DMF. The temperature dependence of the kinetics leads to unusually low preexponential factors for this series. The low preexponential factor is interpreted in terms of a nonadiabatic effect resulting from weak electronic coupling between the reactant and product surfaces. Finally, the data are discussed in the context of recent advances of dissociative electron transfer reported by Savéant and by German and Kuznestov. In total the results suggest that these peroxides undergo a nonadiabatic dissociative electron transfer and represent the first reported class of compounds where this effect is reported.

Introduction

Electron transfer (ET) to an organic molecule (A−B) is often accompanied by fragmentation with the formation of a radical, A$^{\bullet}$, and an anion, B^{-}.[2−4] This process can occur either via a stepwise mechanism with an intermediate radical anion (eqs 1 and 2) or via a concerted pathway in which ET and bond breaking occur in one step (eq 3). Work by Savéant and co-workers have laid the foundation of our understanding of the concerted mechanism in comparison with the corresponding stepwise process.[5] The Savéant model is based on a Morse potential for the A−B bond and the assumption that the dissociative potential for the product state is the same as the repulsive part of the reactant potential.[6] This leads to an expression relating the activation free energy, $\Delta G^{\ddagger}$, to the reaction free energy, $\Delta G°$, (eq 4) that is equal to the well-known Marcus equation[7] with the exception that the intrinsic barrier ($\Delta G_0^{\ddagger}$) contains contributions from the bond dissociation enthalpy of the A−B bond (BDE) in addition to the reorganization energy (λ), which is often separated into the solvent (λ_s) and inner reorganization (λ_i) energies (where the latter term does not include the contribution of the mode of the A−B bond).

$$\mathrm{A{-}B} + \mathrm{e}^{-} \rightleftharpoons \mathrm{A{-}B}^{\bullet -} \tag{1}$$

$$\mathrm{A{-}B}^{\bullet -} \rightarrow \mathrm{A}^{\bullet} + \mathrm{B}^{-} \tag{2}$$

$$\mathrm{A{-}B} + \mathrm{e}^{-} \rightarrow \mathrm{A}^{\bullet} + \mathrm{B}^{-} \tag{3}$$

$$\Delta G^{\ddagger} = \Delta G_0^{\ddagger}\left(1 + \frac{\Delta G°}{4\Delta G_0^{\ddagger}}\right)^2 \tag{4}$$

$$\Delta G_0^{\ddagger} = \frac{\mathrm{BDE} + \lambda}{4} \tag{5}$$

The model has been validated, in particular, by a number of studies of both heterogeneous and homogeneous reduction of carbon−halogen bonds.[2,3] We applied this model in our study of the dissociative reduction of oxygen−oxygen bonds of alkyl

[†] The University of Western Ontario.
[‡] Università di Padova.
[§] National Research Council of Canada.

(1) Issued as NRCC Publication No. 42182.
(2) Savéant, J.-M. *Adv. Phys. Org. Chem.* **1990**, *26*, 1.
(3) Savéant, J.-M. *Acc. Chem. Res.* **1993**, *26*, 455.
(4) (a) Saeva, F. D. In *Topics in Current Chemistry*; Mattay, J., Ed.; Springer-Verlag: Berlin, 1990; Vol. 156, p 59. (b) Schuster, G. B. In *Advances in Electron Transfer Chemistry*; Mariano, P. S., Ed.; JAI Press: Greenwich, CT, 1991; Vol. 1, p 163. (c) Maslak, P. In *Topics in Current Chemistry*; Mattay, J., Ed.; Springer-Verlag: Berlin, 1993; Vol. 168, p 1. (d) Gaillard, E. R.; Whitten, D. G. *Acc. Chem. Res.* **1996**, *29*, 292.
(5) Savéant, J.-M. In *Advances in Electron Transfer Chemistry*; Mariano, P. S., Ed.; JAI Press: Greenwich, CT, 1994; Vol. 4, p 53.
(6) Savéant, J.-M. *J. Am. Chem. Soc.* **1987**, *109*, 6788.
(7) Marcus, R. A.; Sutin, N. *Biochim. Biophys. Acta* **1985**, *811*, 265.

10.1021/ja9906148 CCC: $18.00
Published on Web 07/23/1999

peroxides.[8] In that study we showed that the electrochemical reduction of alkyl peroxides is in agreement with a concerted mechanism. By use of the potential dependence of the transfer coefficient, α, both the intrinsic barriers and bond dissociation energies for O−O bond cleavage could be derived. Values for the heterogeneous intrinsic barrier and the BDE of the peroxide of 10−13 and 34−37 kcal mol^{-1}, respectively, were obtained and depended to some extent on the structure. We applied the same method to derive the standard potential for the concerted reduction of biologically relevant endoperoxides.[9]

We also reported rate constants for the homogeneous reduction of di-*tert*-butyl peroxide (DTBP) in acetonitrile (MeCN) and *N*,*N*-dimethylformamide (DMF) in a previous study.[10] At that time we reported that the Savéant model overestimated the actual rate constants by almost 4 orders of magnitude. We suggested that steric inhibition was partly responsible for this discrepancy due to the exponential decrease of the electronic coupling between reactant and product states. The bulky *tert*-butyl groups block access of the reductants to the O−O bond. The remainder of the discrepancy was attributed to a nonadiabatic effect resulting from intrinsically poor electronic coupling between the reactant and product surfaces.

A recent paper by Savéant and co-workers points out that in our original report we used the bond dissociation *free* energy (BDFE) rather than the BDE in our estimate of the intrinsic barrier.[11] As we will see, this has the effect of decreasing the rate constants predicted by the model by about 1.5 orders of magnitude. Thus, the discrepancy between the model and the experiment is now only 2.0−2.5 orders of magnitude. Savéant and co-workers go on to develop an extension of their model, which takes cage and entropy effects into account. This paper represents a key advance in how one should think about the concerted processes. In essence, it points out that the available thermodynamic driving force, $-\Delta G°$, provides information that relates energies of solvent-separated reactants to solvent-separated products (eq 3 where e$^-$ is either the electrode or a homogeneous reductant). However, the reaction for which the measured activation energy is relevant is one in which the reactants are solvent-separated species while the products are formed in a solvent cage (eq 6). The products diffuse apart and become independently solvated in a separate step with an activation barrier that is much less than the barrier for the ET. To solve this complex problem, it was assumed that the entropy change associated with the formation of the fragments in a cage, $\Delta S°_{F,C}$, is a fraction (ϕ) of the overall entropy change, $\Delta S°_F$. It was further assumed that the entropy changes linearly from reactants to products leading to eqs 7−9, which can be fit iteratively to the experimental data (H_{RP} is the avoided crossing energy and $\Delta S°_S$ is the change in solvation entropy associated with the reaction). The overall entropy change is simply $\Delta S°_S + \Delta S°_F$. Finally, the transfer coefficient, α, at a given driving force can be calculated (eq 10). In eqs 7, 8, and 10, the λ_i term has been neglected; this seems to be a reasonable approximation for strongly dissociative ETs, i.e., when dealing with aromatic electron donors and with acceptors where the breaking bond stretches along the reaction coordinate without significant rearrangement of the rest of the molecular framework.

$$A-B + D^{\bullet -} \rightarrow (A^{\bullet}B^{-}D)_{sol} \quad (6)$$

$$\Delta G^{\ddagger} = \frac{BDE + \lambda_S}{4}\left(1 + \frac{\Delta G°_C}{BDE + \lambda_S}\right)^2 - \frac{(T\Delta S°_F\phi)^2}{4\,BDE} - H_{RP} \quad (7)$$

$$\Delta S^{\ddagger} = \frac{1}{2}\left(1 + \frac{\Delta G°_C}{BDE + \lambda_S}\right)(\Delta S°_F\phi + \Delta S°_S) + \frac{T\Delta S°_F\phi}{2\,BDE} \quad (8)$$

$$\Delta G°_C = \Delta G° + T\Delta S°_F(1 - \phi) \quad (9)$$

$$\alpha = \frac{1}{2}\left(1 + \frac{\Delta G°_C}{BDE + \lambda_S}\right) \quad (10)$$

In this paper we reexamine the concerted reduction of DTBP in the context of the cage and nonadiabatic effects. By use of available thermodynamic data, the activation parameters are predicted using Savéant's most recent model.[11] Experimental activation parameters for the reduction of DTBP by five mediators that cover a range of 0.4 eV in driving force are obtained from the temperature dependence of the kinetics between 50 and −30 °C in DMF. In addition, the role of steric effects on the kinetics of these processes is evaluated by comparison of DTBP with the heterogeneous reduction of di-*n*-butyl peroxide (DNBP) and the homogeneous reduction of dicumyl peroxide (DCP). Finally, these data are discussed with respect to the more generalized quantum mechanical theory of dissociative electron transfer proposed by German and Kuznetsov.[12]

Experimental Section

Chemicals. *N*,*N*-Dimethylformamide (Janssen, 99%) was purified as previously described.[8] Acetonitrile (BDH) was distilled over CaH_2 and stored under an argon atmosphere. The supporting electrolyte was tetraethylammonium perchlorate, TEAP, (Fluka) that was recrystallized twice from ethanol and dried at 60 °C under vacuum. Di-*tert*-butylperoxide (Aldrich), dicumyl peroxide (Aldrich), acetanilide (Janssen), fluorene (Janssen), cumyl alcohol (Aldrich), chrysene (Aldrich), 7,8-benzoquinoline (Aldrich), pyrene (Fluka), anthracene (Erba), 9,-10-diphenylanthracene (Aldrich), fluoranthene (Ega), perylene (Fluka), acenaphthylene (Fluka), naphthacene (Fluka), naphthalene (Aldrich), benzophenone (Erba), 2,2,2-trifluoroethanol (Aldrich), and 2,6-di-*tert*-butyl phenol were of high purity and either used as received or purified prior to use. 4-Methyl-azobenzene and 4-methyl-4′-ethoxyazobenzene were synthesized as previously described.[13] The synthesis of di-*n*-butyl peroxide was carried out by slight modifications of a literature method.[14]

Electrochemistry. The glassy carbon (Tokai GC-20) electrode was prepared and activated before each measurement as previously described.[8] The electrode area, necessary to calculate the diffusion coefficients, was determined through the limiting convolution[15] currents of ferrocene; the diffusion coefficient of ferrocene is 1.13×10^{-5} and 2.38×10^{-5} cm^2 s^{-1} in DMF and MeCN, respectively.[16] The reference electrode was Ag/AgCl, calibrated after each experiment against the ferrocene/ferricenium couple. In the presence of 0.1 M TEAP, we measured $E°_{Fc/Fc+}$ to be 0.475 and 0.450 V versus the KCl saturated calomel electrode (SCE) in DMF and in MeCN, respectively. All potentials values are reported versus SCE. The counter electrode was a 1 cm^2 Pt plate.

(8) Antonello, S.; Musumeci, M.; Wayner, D. D. M.; Maran, F. *J. Am. Chem. Soc.* **1997**, *119*, 9541.

(9) (a) Workentin, M. S.; Donkers. R. L. *J. Am. Chem. Soc.* **1998**, *120*, 2664. (b) Donkers, R. L.; Workentin, M. S. *J. Phys. Chem. B* **1998**, *102*, 4061.

(10) Workentin, M. S.; Maran, F.; Wayner, D. D. M. *J. Am. Chem. Soc.* **1995**, *117*, 2120.

(11) Andrieux, C. P.; Savéant, J.-M.; Tardy, C. *J. Am. Chem. Soc.* **1998**, *120*, 4167.

(12) (a) German, E. D.; Kuznetsov, A. M. *J. Phys. Chem.* **1994**, *98*, 6120. (b) German, E. D.; Kuznetsov, A. M.; Tikhomirov, V. A. *J. Phys. Chem.* **1995**, *99*, 9095.

(13) Severin, M. G.; Arévalo, M. C.; Maran, F.; Vianello, E. *J. Phys. Chem.* **1993**, *97*, 150.

(14) Foglia, T. A.; Silbert, L. S. *Synthesis* **1992**, 545.

(15) Imbeaux, J. C.; Savéant, J.-M. *J. Electroanal. Chem.* **1973**, *44*, 169.

(16) Curtis, N.; Donkers, R. L.; Leaist, D. G.; Maran, F.; Workentin, M. S. Manuscript in preparation.

Electrochemical measurements were conducted in an all-glass cell thermostated at the required temperature. For the temperature dependence studies the temperature was controlled using a VWR Scientific model 1150A constant temperature circulator; the cell was allowed to equilibrate for 30 min at each temperature. An EG&G-PARC 173/179 potentiostat−digital coulometer, EG&G-PARC 175 universal programmer, Nicolet 3091 12-bit resolution digital oscilloscope, and Amel 863 *X/Y* pen recorder or an EG&G-PARC 283 potentiostat interfaced to a computer were used. In all cases, *iR* compensation was employed. Convolution analyses were carried out on digitalized, background-subtracted voltammetric curves as previously described.[8] Digital simulations of the cyclic voltammetry curves were performed by using the DigiSim 2.1 software by Bioanalytical Systems Inc.

Controlled Potential Electrolysis and HPLC Analysis. Controlled potential bulk electrolyses were performed in a divided cell using a mercury pool cathode or a platinum grid as the working electrode. Electrolyses were carried out at 25 °C in 10 mM solutions continuously deoxygenated with argon at a constant potential just beyond the voltammetric reduction peak. The electron consumption was determined after the electrolysis current dropped to 1−2% of its original value. Some electrolyses were carried out also in the presence of added weak acids (trifluoroethanol, fluorene, acetanilide, or 2,6-di-*tert*-butylphenol). The indirect controlled potential electrolyses were carried out by reducing the mediator (1 mM perylene) in the presence of the peroxide (2 mM). The extent of the catalyzed reduction was followed by cyclic voltammetry and by taking aliquots of the partially electrolyzed solution at given values of the charge consumed. Each aliquot was divided into two samples one of which was acidified. In all cases, HPLC analysis gave the same result. The indirect electrolyses were arbitrarily halted after theoretical destruction of half of the peroxide, based on the consumption of 2 F mol^{-1}.

HPLC was performed using a Perkin-Elmer series 4 liquid chromatograph (column: Sperisorb ODS2 C_{18}, 5 μm, 4.6 mm × 15 cm), equipped with a UV LC-85 variable-wavelength detector and a Perkin-Elmer 3700 data station for chromatogram analysis. The detection wavelength was 220 nm. The eluting solution was programmed: 2 min at 50% acetonitrile/50% water, 1 min to reach 90% acetonitrile/water, and then the same eluent was maintained for 7 min. The flow rate was 2.0 mL/min. Quantitative analysis was based on peak areas that were calibrated using authentic samples. Naphthalene was used as an internal standard.

Results and Discussion

Voltammetric Behavior and Coulometry. The reduction of DTBP and DCP (and other dialkyl peroxides) was previously studied in DMF/0.1 M tetra-*n*-butylammonium perchlorate (TBAP).[8] In DMF or MeCN at either a glassy carbon or mercury electrode, only one electrochemically irreversible reduction peak is observed. Results for DNBP were qualitatively similar, although the voltammetry at the mercury electrode for this compound was not as well defined. The reduction of the peroxides is essentially independent of the electrolyte, as verified by changing TBAP with TEAP. The latter was the electrolyte of choice in the present study. The peak potential (E_p) values measured at 25 °C at a scan rate (υ) of 0.2 V s^{-1} are given in Table 1. For comparison, the values of the transfer coefficient α, obtained from the corresponding peak width, $\Delta E_{p/2} = 1.857RT/(F/\alpha)$,[17] and from the scan rate dependence of the irreversible peak, $\partial E_p/(\partial \log \upsilon) = 1.15\ RT/(F/\alpha)$,[17] are also reported. Weak acids capable of protonating the product alkoxides[8] (trifluoroethanol, fluorene, acetanilide, and 2,6-di-*tert*-butylphenol with $pK_a^{DMF} = 24.1$, 23.3, 22.3, and 17.7, respectively)[18] had no effect in either solvent on both E_p and the peak current, i_p. The i_p values, or the limiting convolution currents, are essentially independent of the solvent after correction for solvent viscosity.[19,20]

Table 1. Cyclic Voltammetric Data for the Reduction of DTBP, DCP, and DNBP at the Glassy Carbon Electrode (0.2 V s^{-1}, T = 25 °C) and Electrolysis Data for the Same Peroxides, Both in the Absence and Presence of Acids

compound	solvent[a]	E_p (V)	α^b	α^c	n (F mol^{-1}) no acid	n (F mol^{-1}) with acid
DTBP	DMF	−2.50	0.254	0.231	1.9	1.9[d]
DTBP	MeCN	−2.53	0.236	0.228	2.0	2.0[d]
DCP	DMF	−2.10	0.277	0.250	2.0	2.0[d]
DCP	MeCN	−2.07	0.261	0.258	2.0	2.0[e]
DNBP	DMF	−2.09	0.244	0.210	0.9	1.4[d]
DNBP	MeCN	−2.08	0.260	0.234	0.9	2.0[f]

[a] 0.1 M TEAP. [b] From $\Delta E_{p/2} = 1.857RT/(F\alpha)$ (ref 17). [c] From $\partial E_p/\partial \log \upsilon = 1.15RT/(F\alpha)$ (ref 17). [d] Acetanilide. [e] 2,6-Di-*tert*-butyl-4-methylphenol. [f] 2,2,2-Trifluoroethanol.

Electrolyses of DTBP, DCP, and DNBP were carried out at a mercury pool cathode (or platinum grid), under magnetic stirring, as described in the Experimental Section. The number of electrons consumed, *n*, in the absence and presence of acid is summarized in Table 1. With DCP these values were verified by monitoring the formation (HPLC) of 2-phenyl-2-propanol: 1.9 (DMF, no acid), 1.8 (MeCN, no acid), 1.9 equiv (MeCN, acid). For DNBP the low electron consumption in the absence of acid is presumably due to the known slow base-induced decomposition of the peroxide and other possible competing reactions (vide infra) that are not significant on the cyclic voltammetry (CV) time scale.[21]

The two-electron stoichiometry and the concerted nature of the initial ET bond breaking step[8] are in agreement with the reaction sequence outlined in eqs 11 and 12, where the alkoxy radical produced in the dissociative reduction is reduced, providing an overall stoichiometry shown in eq 13.

$$RO{-}OR + e^- \rightarrow RO^\bullet + RO^- \quad (11)$$

$$RO^\bullet + e^- \rightarrow RO^- \quad (12)$$

$$RO{-}OR + 2e^- \rightarrow 2\ RO^- \quad (13)$$

Two macroelectrolyses were carried out in both solvents by making use of the principles of homogeneous electrocatalysis.[22] The radical anion of an aromatic compound is generated by electrolysis at a potential negative to the reduction peak of the mediator itself but more positive than the reduction potential

(17) (a) Nicholson, R. S.; Shain, I. *Anal. Chem.* **1964**, *36*, 706. (b) Bard, A. J.; Faulkner, L. R. *Electrochemical Methods, Fundamentals and Applications*; Wiley: New York, 1980.

(18) (a) Bordwell, F. G. *Acc. Chem. Res.* **1988**, *21*, 456. (b) Maran, F.; Celadon, D.; Severin, M. G.; Vianello, E. *J. Am. Chem. Soc.* **1991**, *113*, 9320.

(19) The limiting convolution current, I_l, is defined as $I_l = nFAD^{1/2}C^*$, where *n* is the overall electron consumption, *D* the diffusion coefficient, and C^* the substrate concentration. I_l is the plateau value reached by the convolution current *I* when the applied potential is negative enough. *I* is related to the actual current *i* through the convolution integral[15]

$$I = \pi^{-1/2}\int_0^t \frac{i(u)}{(t-u)^{1/2}}\,du$$

For example, the diffusion coefficient of DCP, determined by convolution voltammetry, is 7.34×10^{-6} and 1.86×10^{-5} $cm^2\ s^{-1}$ in DMF and MeCN, respectively. This leads to a ratio of 2.53, in good agreement with the ratio between the viscosity of DMF and that of MeCN, 0.796/0.344 = 2.31,[20] and thus with the Stokes−Einstein relation. Analogous results are obtained with the other peroxides. This is relevant because it means that the number of exchanged electrons is the same in both solvents, within error.

(20) Riddick, J. A.; Bunger, W. B.; Sakano, T. K. *Organic Solvents, Physical Properties and Methods of Purification*, 4th ed.; Weissberger, A., Ed.; Techniques of Chemistry II; John Wiley and Sons: New York, 1986.

(21) *Organic Peroxides*; Ando, W., Ed.; Wiley: New York, 1992.

(22) (a) Andrieux, C. P.; Blocman, C.; Dumas-Bouchiat, J. M.; M'Halla, F.; Savéant J.-M. *J. Electroanal. Chem.* **1980**, *113*, 19. (b) Andrieux, C. P.; Savéant J.-M. *J. Electroanal. Chem.* **1986**, *205*, 43.

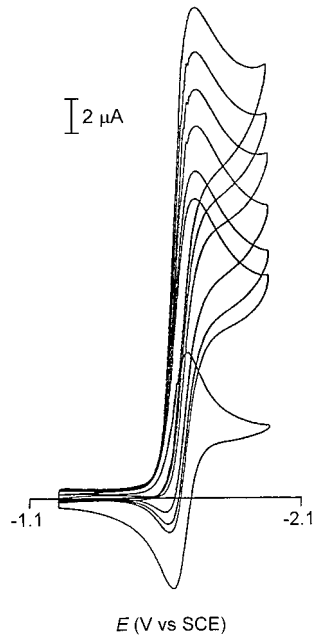

Figure 1. Cyclic voltammetry curves taken during the macroreduction of DCP (2 mM) mediated by perylene (1 mM) in MeCN/0.1 M TEAP, at 0.2 V s^{-1}. The curves (top to bottom) correspond to an electron consumption of 0, 0.2, 0.4, 0.6, 0.8, 1.0, and 2.0 F mol^{-1}. The last curve is coincident to that of perylene in the absence of DCP. The electrode was glassy carbon, and $T = 25$ °C.

of the substrate (in these cases the peroxide). For example, we used perylene as the mediator and focused on DCP. The evolution of the electrolysis was monitored by both cyclic voltammetry and HPLC. The reduction peak of perylene in the absence and in the presence of 2 equiv of DCP is shown in Figure 1. The presence of the peroxide causes the peak current of perylene (the donor, D) to increase because of the catalytic cycle outlined in eqs 14−16. Figure 1 also illustrates how the voltammetric wave changes progressively after the passage of small quantities of charge, each wave corresponding to 0.2 F mol^{-1}. HPLC reflects the evolution toward the overall stoichiometry of eq 13. For every equivalent of DCP consumed, 2 equiv of cumyl alcohol is produced. No change in the concentration of the perylene mediator or the formation of other species was observed, indicating that no coupling (such as the reaction in eq 17) similar to that observed in the reduction of alkyl and benzyl halides is observed. It is also noteworthy that in the product study for the reduction of DCP no acetophenone was observed. Acetophenone would be formed from the known β-scission of the cumyloxy radical (CumO•), before its ET reduction (eq 16),[23] suggesting that the latter reaction must be close to diffusion-controlled.

$$D + e^- \rightleftarrows D^{\bullet -} \quad (14)$$

$$D^{\bullet -} + RO{-}OR \rightarrow RO^{\bullet} + RO^- + D \quad (15)$$

$$D^{\bullet -} + RO^{\bullet} \rightarrow RO^- + D \quad (16)$$

$$D^{\bullet -} + R^{\bullet} \rightarrow DR^- \quad (17)$$

For DCP in MeCN, electrolysis requires 2 F mol^{-1}, but only 1.4 F mol^{-1} is consumed in the corresponding indirect electrolysis in DMF. The difference between these two values is likely related to the fast H atom abstraction from DMF by CumO•. Decay of the radical (lifetime is 60 ns in DMF compared to 1.6 μs in MeCN) would have the consequence of lowering the overall electron stoichiometry. H atom abstraction would also be consistent with similar results obtained from the mediated electroreduction of DTBP.[24] The difference between the direct and indirect electrolyses of DCP in DMF is related to the dissociative nature of the initial ET. Thus, in the direct electrolysis the cumyloxy radical is generated at the electrode surface where it is immediately reduced. Likewise, the lower electron stoichiometry for DNBP in DMF can be attributed to H-abstraction reactions with solvent and the peroxide itself.

Dissociative Standard Potential of Peroxides. Dissociative ETs (eq 3) are irreversible reactions, and therefore, their standard potentials ($E^\circ_{AB/A^\bullet,B-}$) cannot be measured directly. However, they can be estimated in two ways: (i) by thermochemical calculations or (ii) by kinetic ET data coupled with the use of the quadratic activation-driving force relationship 4, as shown very recently for different dissociative-type compounds.[8,9,25,26] The first approach is based on the thermochemical cycle outlined below (eq 18).[27]

$$\begin{aligned} & AB \rightleftarrows A^\bullet + B^\bullet && \text{BDFE} \\ & B^\bullet + e^- \rightleftarrows B^- && -FE^\circ_{B^\bullet/B-} \\ \text{net:}\quad & AB + e^- \rightleftarrows A^\bullet + B^- && -FE^\circ_{AB/A^\bullet,B-} \\ & E^\circ_{AB/A^\bullet,B-} = E^\circ_{B^\bullet/B-} && -\text{BDFE}/F \end{aligned} \quad (18)$$

Peroxides are characterized by low bond dissociation enthalpies, BDE, of about 30−40 kcal mol^{-1}.[28] Some of the reported data are obtained from the gas-phase kinetics and must be converted to solution BDFEs by an appropriate entropy correction (vide infra).[29] Alternatively, BDFEs can be calculated from the solution homolysis equilibrium constant obtained from the decomposition rate constant and the rate constant for the dimerization of RO• radicals, k_d. For *t*-BuO• or CumO•, $k_d = 2 \times 10^9$ M^{-1} s^{-1} at 25 °C.[30] For DTBP, reported BDE values are 37.4, 38.0, and 36.4 kcal mol^{-1}, leading to an average BDFE value of 28.8 kcal mol^{-1} ($\Delta S^\circ = 28.5$ cal mol^{-1} K^{-1} [29]), which is close to the value based on the equilibrium constant of 28.7 kcal mol^{-1}. The equilibrium constant K for the homolysis of DTBP was determined from the extrapolated forward rate constant, 1.66×10^{-12} s^{-1} [32] and the k_d value given above. For DCP, a similar analysis leads to BDFE = 27.2 kcal mol^{-1},[33] which also agrees with the value of 27.7 kcal mol^{-1} obtained by convolution.[8] The latter value will be used in the following discussion. The BDFE of DNBP is not known but can be estimated by comparison with the BDE of di-*n*-propyl (37.1 and 36.5 kcal mol^{-1}), diisopropyl (37.7 kcal mol^{-1})[31b,34] and

(23) Avila, D. V.; Brown, C. E.; Ingold, K. U.; Lusztyk, J. *J. Am. Chem. Soc.* **1993,** *115*, 466.
(24) Kjær, N. T.; Lund, H. *Acta Chem. Scand.* **1995**, *49*, 848.
(25) Antonello, S.; Maran, F. *J. Am. Chem. Soc.* **1997**, *119*, 12595.
(26) Antonello, S.; Maran, F. *J. Am. Chem. Soc.* **1998**, *120*, 5713.
(27) Wayner, D. D. M.; Parker, V. D. *Acc. Chem. Res.* **1993**, *26*, 287.
(28) Baldwin, A. C. In *The Chemistry of Peroxides*; Patai, S., Ed.; Wiley: New York, 1983; p 97.
(29) Benson, S. W. *Thermochemical Kinetics*, 2nd ed.; Wiley: New York, 1976.
(30) Wong, S. K. *Int. J. Chem. Kinet.* **1981**, *13*, 433.
(31) (a) Batt, L.; Benson, S. W. *J. Chem. Phys.* **1962**, *36*, 895. (b) Batt, L.; Christie, K.; Milne, R. T.; Summers, A. *Int. J. Chem. Kinet.* **1974**, *6*, 877. (c) Lewis, D. K. *Can. J. Chem.* **1976**, *54*, 581.
(32) Matsugo, S.; Saito, I. In *Organic Peroxides*; Ando, W., Ed.; Wiley: New York, 1992.
(33) Denisov, E. T. In *Liquid Phase Reaction Rate Constants*; Plenum: New York, 1974.
(34) Benson, S. W. *J. Chem. Phys.* **1964**, *40*, 1007.

Table 2. Rate Constants for the Homogeneous Electron Transfer (k_{hom}) from Electrogenerated Radical Anion Donors to DTBP at 25 °C

donor (D)	$E^\circ_{D/D^{\bullet-}}$ (V) (DMF)	ΔG° (eV)[a] (DMF)	log k_{hom} (DMF)	$E^\circ_{D/D^{\bullet-}}$ (V) (MeCN)	ΔG° (eV)[b] (MeCN)	log k_{hom} (MeCN)
chrysene	−2.245	−0.765	5.11	−2.266	−0.716	4.87
7,8-benzoquinoline	−2.170	−0.690	4.68	−2.150	−0.600	4.51
isoquinoline	−2.092	−0.612	4.39			
pyrene	−2.004	−0.524	4.05	−2.008	−0.458	3.82
anthracene	−1.928	−0.448	3.31	−1.965	−0.415	3.09
9,10-diphenylanthracene	−1.837	−0.357	2.89	−1.873	−0.323	2.85
fluoranthene	−1.729	−0.249	2.15	−1.762	−0.212	2.03
perylene	−1.645	−0.165	1.82	−1.670	−0.120	1.67
acenaphthylene	−1.633	−0.153	1.26	−1.653	−0.103	1.04
naphthacene	−1.545	−0.065	0.91			

[a] $E^\circ_{t\text{-BuOOBu}-t/t\text{-BuO}\bullet,t\text{-BuO}-}$(DMF) = −1.48 V. [b] $E^\circ_{t\text{-BuOOBu}-t/t\text{-BuO}\bullet,t\text{-BuO}-}$(MeCN) = −1.55 V.

di-*sec*-butyl peroxide (36.4 kcal mol^{-1}).[35] The BDE of DNBP can therefore be estimated to be about 36.8 kcal mol^{-1}, which leads to an estimate of 28.3 kcal mol^{-1} for the BDFE.

The value of $E^\circ_{B^\bullet/B-}$ can be obtained either from thermochemical calculations or from voltammetry of RO$^\bullet$ or RO$^-$.[36] The thermochemical approach was chosen for the *t*-BuO$^\bullet$/*t*-BuO$^-$ and *n*-BuO$^\bullet$/*n*-BuO$^-$ couples, since the voltammetric wave for the reduction of *t*-BuO$^\bullet$ is ill-defined and the pK_a's of *n*-BuO$^-$ and *t*-BuO$^-$ are too high to be produced in solution at a sufficiently high concentration (even in carefully purified solvents the concentration of water, a stronger proton donor than butanol by about 1 pK_a unit,[18a] is still at millimolar levels). The standard potentials for the *t*-BuO$^\bullet$/*t*-BuO$^-$ and *n*-BuO$^\bullet$/*n*-BuO$^-$ couples were calculated using eq 19, which is derived from the thermochemical cycle below.

$$\mathrm{RO}^\bullet + \mathrm{H}^\bullet \rightleftarrows \mathrm{ROH} \qquad -\mathrm{BDFE}$$

$$\mathrm{ROH} \rightleftarrows \mathrm{RO}^- + \mathrm{H}^+ \qquad 2.303RT(\mathrm{p}K_a)$$

$$\mathrm{H}^+ + \mathrm{e}^- \rightleftarrows \mathrm{H}^\bullet \qquad -FE^\circ_{H+/H\bullet}$$

$$\text{net:} \quad \mathrm{RO}^\bullet + \mathrm{e}^- \rightleftarrows \mathrm{RO}^- \qquad -FE^\circ_{RO\bullet/RO-}$$

$$E^\circ_{t\text{-BuO}\bullet/t\text{-BuO}-} = \mathrm{BDFE}/F - 2.303(RT/F)\mathrm{p}K_a + E^\circ_{H+/H\bullet} \quad (19)$$

Values for the BDFE of RO−H can be estimated from gas-phase data, correcting for solvation of the proton.[27,37] pK_a values for *tert*-butyl alcohol were calculated using the value reported for dimethyl sulfoxide, 32.2,[18a] and one of the two equations pK_a(DMF) = 1.56 + 0.96 pK_a(Me$_2$SO) and pK_a(MeCN) = 7.10 + 1.17 pK_a(Me$_2$SO).[18b,10,] Accordingly, the pK_a values of *t*-BuOH are estimated to be 32.5 and 44.8 and those of *n*-BuOH are estimated to be and 30.4 and 42.3 in DMF and MeCN, respectively. The $E^\circ_{H+/H\bullet}$ values are −2.69 and −2.01 V vs SCE in DMF and MeCN, respectively,[27] leading to the following standard potentials: $E^\circ_{t\text{-BuO}\bullet/t\text{-BuO}-}$(DMF) = −0.23 V; $E^\circ_{t\text{-BuO}\bullet/t\text{-BuO}-}$(MeCN) = −0.30 V; $E^\circ_{n\text{-BuO}\bullet/n\text{-BuO}-}$(DMF) = −0.15 V; $E^\circ_{n\text{-BuO}\bullet/n\text{-BuO}-}$(MeCN) = −0.20 V.

By contrast, the standard potential for the CumO$^\bullet$/CumO$^-$ couple ($E^\circ_{B\bullet/B-}$) can be calculated from voltammetric measurements on the alkoxide (prepared separately or by reduction of the DCP). This is because cumyl alcohol is more acidic than water by 2−3 pK_a units.[8] In DMF, an irreversible oxidation peak that can be attributed to the anion CumO$^-$ is detectable for $v > 0.5$ V s^{-1} and is well defined for $v \geq 2$ V s^{-1}. The scan rate dependence of this peak was measured between 0.5 and 50 V s^{-1}. The one-electron oxidation appears to be sufficiently fast in DMF to analyze the peak in order to obtain the desired $E^\circ_{B\bullet/B-}$ in this solvent. The voltammetric data are consistent with a first-order reaction consuming the electrogenerated species (i.e., direct hydrogen atom abstraction from the solvent as the major reaction channel).[17] The constant value of $i_p/v^{1/2}$ is consistent with having a steady concentration of CumO$^-$ in the diffusion layer near the electrode. By use of literature values for the rate constants of the followup reactions,[17,27] a value of $E^\circ_{CumO\bullet/CumO-} = -0.12 \pm 0.05$ V was obtained. This value is reasonable in comparison with the above thermochemical calculations for the *t*-BuO$^\bullet$/*t*-BuO$^-$ and *n*-BuO$^\bullet$/*n*-BuO$^-$ couples as well as the experimental E° for the Ph$_3$CO$^\bullet$/Ph$_3$CO$^-$ couple, −0.03 V.[8] In MeCN, the quality of the E_p data prevented a quantitative calculation. Qualitatively, however, the experimental data are consistent with a similar potential shift calculated for *t*-BuO$^-$ (0.07 V on going from DMF to MeCN). Accordingly, $E^\circ_{CumO\bullet/CumO-}$(DMF) = −0.12 V and $E^\circ_{CumO\bullet/CumO-}$(MeCN) = −0.19 V. By use of the above values, the corresponding dissociative E° values can be calculated (± 0.05−0.1 V):

$$E^\circ_{t\text{-BuOOBu}-t/t\text{-BuO}\bullet,t\text{-BuO}-}(\mathrm{DMF}) = -1.48 \text{ V}$$

$$E^\circ_{t\text{-BuOOBu}-t/t\text{-BuO}\bullet,t\text{-BuO}-}(\mathrm{MeCN}) = -1.55 \text{ V}$$

$$E^\circ_{n\text{-BuOOBu}-n/n\text{-BuO}\bullet,n\text{-BuO}-}(\mathrm{DMF}) = -1.38 \text{ V}$$

$$E^\circ_{n\text{-BuOOBu}-n/n\text{-BuO}\bullet,n\text{-BuO}-}(\mathrm{MeCN}) = -1.43 \text{ V}$$

$$E^\circ_{\mathrm{CumOOCum/CumO}\bullet,\mathrm{CumO}-}(\mathrm{DMF}) = -1.32 \text{ V}$$

$$E^\circ_{\mathrm{CumOOCum/CumO}\bullet,\mathrm{CumO}-}(\mathrm{MeCN}) = -1.39 \text{ V}$$

Electron Transfer to DTBP and DCP. The homogeneous ET to DTBP in both DMF and MeCN was previously reported, and the rate (the k_{hom} values pertains to the dissociative ET of eq 14) and driving force data are reported in Table 2. A similar study was carried out for DCP, again in both solvents. The indirect reduction was accomplished by homogeneous redox catalysis using electrogenerated radical anions as homogeneous electron donors.[22] As already mentioned, the reversible reduction peak of the mediator is transformed into a chemically irrevers-

(35) Walker, R. F.; Phillips, L. *J. Chem. Soc. A* **1968**, 2103.

(36) In principle it is possible to generate a constant concentration of these radicals and to study their reduction by photomodulated voltammetry, as previously done with many other radicals (Wayner, D. D. M.; McPhee, D. J.; Griller, D. *J. Am. Chem. Soc.* **1988**, *110*, 132), but the electrochemistry is ill-defined.

(37) *NIST Standard Reference Database 25*; NIST Structures and Properties Database and Estimation Program, U.S. Department of Commerce: Gaithersburg, MD, 1991.

(38) Izutzu, K. *Acid−Base Dissociation Constants in Dipolar Aprotic Solvents*; Chemical Data Series 35; Blackwell Scientific Publications: Oxford, 1990.

Table 3. Rate Constants for the Homogeneous Electron Transfer (k_{hom}) from Electrogenerated Radical Anion Donors to DCP at 25 °C

donor	$E°_{D/D•-}$ (V) (DMF)	$\Delta G°$ (eV)[a] (DMF)	log k_{hom} (DMF)	$E°_{D/D•-}$ (V) (MeCN)	$\Delta G°$ (eV)[b] (MeCN)	log k_{hom} (MeCN)
anthracene	−1.928	−0.608	4.81	−1.965	−0.575	4.98
9,10-diphenylanthracene	−1.837	−0.517	4.40	−1.873	−0.483	4.35
benzophenone	−1.755	−0.435	3.57			
fluoranthene	−1.729	−0.409	3.81	−1.762	−0.372	3.83
perylene	−1.645	−0.325	3.29	−1.670	−0.280	3.10
acenaphthylene	−1.633	−0.313	2.97	−1.653	−0.263	2.96
naphthacene	−1.545	−0.225	2.54			
terephthalonitrile	−1.545	−0.225	2.67	−1.580	−0.190	2.73
4-methyl-4′-ethoxyazobenzene	−1.485	−0.165	1.63	−1.485	−0.095	1.85
4-methylazobenzene	−1.355	−0.035	0.82	−1.385	+0.005	1.06

[a] $E°_{CumOOCum/CumO•,CumO-}$(DMF) = −1.32 V. [b] $E°_{CumOOCum/CumO•,CumO-}$(MeCN) = −1.39 V.

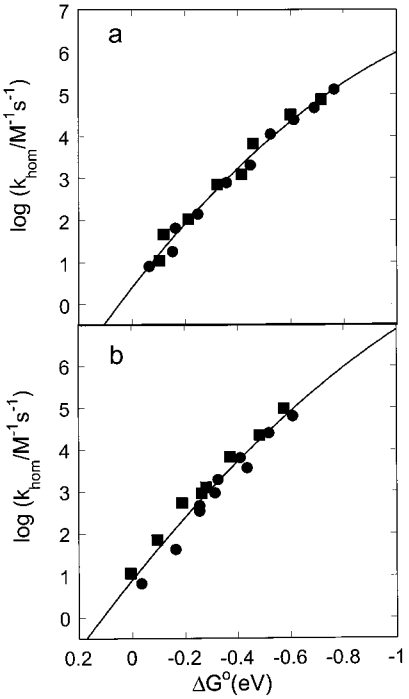

Figure 2. Plot showing the variation in the logarithm of the rate constant for ET, log(k_{hom}), with the driving force, for the homogeneous electron-transfer reactions of a number of aromatic radical anions with (a) DTBP and (b) DCP in DMF (●) and MeCN (■) at 25 °C. The curve is simply a fit to a second-order polynomial.

ible, catalytic peak upon addition of the peroxide (eqs 14−16). The current of the catalytic peak depends on both the scan rate and the concentration of the substrate. Rate constants (scan rate of 0.2−2 V s^{-1} using at least three concentrations of the substrate) were then determined using theoretical curves or by simulation of the experimental voltammograms corresponding to eqs 14−16. Data for DCP from cyclic voltammograms are reported in Table 3. For both peroxides, the uncertainty of the measured k_{hom} values is estimated to be ±10−15%. The proton donors were shown to be mild enough to protonate the alkoxide ions but not the radical anion of the donor and had no effect on the extracted log k_{hom} values.[39] By use of the values of the dissociative standard potentials determined above, log(k_{hom}) for DTBP and DCP can be plotted as a function of the reaction free energy (Figure 2).

One possible complication in the analysis is the consumption of the catalyst by coupling with the DMF-derived radical (which is formed by reaction of *tert*-butoxyl radical with the solvent; eqs 20 and 21).[24]

$$RO^{\bullet} + Me_2NCHO \rightarrow ROH + Me_2NC^{\bullet}O \qquad (20)$$

$$D^{\bullet -} + Me_2NCO^{\bullet} \rightarrow Me_2NC(O)D^{-} \qquad (21)$$

In principle, it should be possible to detect these anions on the positive scan after the catalytic reduction. Although anions of this type are expected to undergo a relatively facile oxidation,[40] no oxidation peak could be detected after indirect reduction of DTBP. However, this does not rule out the possibility that these reactions contribute on the longer electrolysis time scale. Indeed the apparent electron consumption of less than 2 in DMF from the indirect electrolysis of DCP is consistent with this scheme. This effect is almost undetectable at low catalysis rates (relatively high scan rates and/or low substrate concentrations) and was taken into account in the determination of the corresponding k_{hom} values.

Heterogeneous Kinetics for Electron Transfer to DNBP. We were not able to obtain reproducible homogeneous rate constants for the reduction of DNBP, so a comparison between the homogeneous ET kinetics of DNBP and that of DTBP is not possible. This is likely because of the base-catalyzed chemistry induced by ET to DNBP and the complex radical and base-induced peroxide decomposition chemistry that follows. However, equivalent information regarding the effect of steric inhibition of ET to DTBP can be obtained from the kinetics of the heterogeneous ET to the two peroxides. Unfortunately, the reduction of DNBP at a mercury electrode is not well behaved and precludes study on this material (in a sense, this effect may be a result of an increased inner sphere contribution to the less hindered peroxide). This would have simplified the analysis because of the possibility of correcting for the double layer effect, as recently described for the reduction of a series of dialkyl peroxides, including DTBP and DCP.[8] Nevertheless, as already described, the reductions of DNBP and DTBP have standard potentials that differ by only 0.10−0.12 V, and thus, a comparison of the heterogeneous rates at the same driving force (and thus where essentially the same double layer effect pertains) is relevant. For both peroxides, the heterogeneous rate was studied in MeCN/0.1 M TEAP at the glassy carbon electrode by using the convolution analysis approach.[8,15] The convolution analysis relies on a series of steps in which background-subtracted cyclic voltammograms are treated to transform the real current i into a convoluted current I.[19] The two currents i and I, which are functions of the time passed during the experiment, are then combined to obtain the

(39) Evidence for the occurrence of the proton transfer was gained through the observation of the oxidation peak of the conjugate base of the added acid during the positive-going scan following the catalytic reduction (e.g., fluorene, E_{ox} = −0.64 V, or acetanilide, E_{ox} = 0.08 V).

(40) Parker, V. D.; Tilset, M.; Hammerich, O. *J. Am. Chem. Soc.* **1987**, *109*, 7905 and references therein.

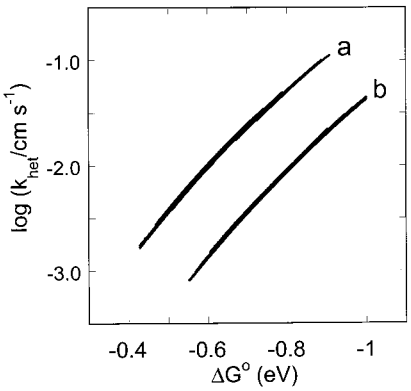

Figure 3. Free energy dependence of the logarithm of the heterogeneous rate constant, $\log(k_{het})$, for the reduction of (a) DNBP and (b) DTBP in MeCN/0.1 M TEAP at the glassy carbon electrode. $T = 25$ °C.

potential dependence of the heterogeneous electron-transfer rate constant, k_{het}. When the electrode process is irreversible, eq 22 applies.

$$\ln k_{het} = \ln D^{1/2} - \ln[(I_l - I(t))/i(t)] \qquad (22)$$

Although we encountered no problems in analyzing the voltammetric curves of DNBP, the reduction of DTBP is close to the solvent/electrolyte discharge with the consequence of complicating the evaluation of I_l. Therefore, we used an approach in which,[8,26] in order to estimate I_l, the rising part of the convolution curves pertaining to different scan rates was fitted by a sigmoid equation. The I_l values thus estimated agreed with each other within 2%, and this was taken as a good indication of the correctness of the procedure employed. The data were finally corrected for the diffusion coefficients, which are 2.45×10^{-5} and 2.47×10^{-5} cm^2 s^{-1} for DNBP and DTBP in MeCN, respectively. A comparison of the plots resulting from the logarithmic analyses pertaining to the two peroxides is shown in Figure 3. It is clear that the heterogeneous kinetics for ET to DNBP is faster than to DTBP at the same driving force by ca. 0.8 $\log(k_{het})$ units. This difference represents the falloff of the rate of reduction of DTBP that can be attributed to the fact that ET must occur over a distance as a result of the O−O σ^* being shielded by the bulky *tert*-butyl groups in DTBP. This effect accounts for only about half of the discrepancy between the experimental results and theoretical prediction (vide infra).

Activation Parameters for Reduction of DTBP. Arrhenius plots of the rate constants for reduction of DTBP by a series of aromatic radical anions (listed in Table 4) are shown in Figure 4. Rate constants were determined by homogeneous redox catalysis in DMF/0.1 M TEAP solution, as described previously. The activation parameters are given in Table 4. We have used $Z = 3 \times 10^{11}$ M^{-1} s^{-1} ($Z = d^2[8\pi k_B T/\mu]^{1/2}$, where d is the encounter distance and μ is the reduced mass) to extract the activation enthalpy and apparent activation entropy from the Arrhenius parameters.

One interesting aspect of the reduction of DTBP is the unusually low Arrhenius preexponential factors, ca. 2.5 orders of magnitude lower than in the reduction of *tert*-butyl bromide.[41] The latter is generally agreed to be an adiabatic ET process. In contrast, the low preexponential factors determined in this study are consistent with a nonadiabatic process as we originally proposed.[10] It also is interesting that the Arrhenius preexponential factor decreases as the driving force increases. A similar trend was reported in the temperature study of the reduction of *tert*-butyl bromide by aromatic radical anions;[41] however, in the reduction of the peroxides the trend is more pronounced. While the low preexponential factors are consistent with our original suggestion of a nonadiabatic process, other explanations should be considered. First, it is possible that the separation of entropy and enthalpy is not precise over the narrow temperature range used in this study. The errors in the determination of the rate constants leads to uncertainties in $\log A$ and E_a of ca. 0.2 and 0.02, respectively; the former is smaller than the observed variation of $\log A$ for the mediators used in this study. Nevertheless, the largest $\log A$ in this study, which is for the slowest mediated reaction, is still significantly smaller than those measured for the *tert*-butyl bromides.[41] Second, there may be subtle temperature changes in the overall electrochemical mechanism that are not evident from macroscale electrolyses. While we do not completely understand the reasons for the observed trend in $\log A$, it is interesting to see if taking account of the cage and entropy effects provides further insights.

To make use of eqs 7−10, values of λ_s, ΔS°_F, and ΔS°_S must be determined or estimated. The λ_s value was determined by using the equation $\lambda_s = 95[(2r_D)^{-1} + (2r_A)^{-1} - (r_D + r_A)^{-1}]$, where D and A are the donor and acceptor, respectively, and the equation is derived from an extensive set of experimental data.[43] An average value of 3.8 Å for r_D was chosen,[43,44] while for DTBP the effective radii approach was used,[5,8] leading to 2.7 Å. This provides $\lambda_s = 15.5$ kcal mol^{-1}. The value of ΔS°_F can be estimated from data in the literature to be 34.6 cal mol^{-1} K^{-1} in the gas phase. Following the suggestion that a correction for the change in the standard state from the gas phase to the liquid phase is required,[11] decreasing the standard entropy of each component by $(R/F)\ln(22.4)$ leads to a final value of $\Delta S^\circ_F = 28.6$ cal mol^{-1} K^{-1}. As expected, this value is close to the value used by Savéant in his estimation of parameters for *tert*-butyl bromide, since most of the entropy change comes from increasing the number of fragments from one to two.

The estimation of ΔS°_S (eq 23) is more difficult, since thermodynamic data for the solvation of alkoxide ions are not available. The last term in eq 23 is the entropy change associated with the conversion of the homogeneous donor into its anion. Savéant has determined this value to be −46 cal mol^{-1} K^{-1} for anthracene. We have assumed that this value is constant for all of the polynuclear aromatic donors used in our study. The entropy of the *tert*-butoxyl radical may be estimated from gas-phase data ($S^\circ_{t-BuO\bullet,DMF} = S^\circ_{t-BuO\bullet,g}$(75.6 cal mol^{-1} K^{-1}) − $[(R/F)\ln(22.4)]$(6.2 cal mol^{-1} K^{-1}) = 69.4 cal mol^{-1} K^{-1}). It is possible to obtain a rough estimate of $S^\circ_{t-BuO-,DMF}$ from the

(41) (a) Lund, H.; Daasbjerg, K.; Lund, T.; Pedersen, S. U. *Acc. Chem Res.* **1995**, *28*, 313. (b) Lund, H.; Daasbjerg, K.; Lund, T.; Occhialini, D.; Pedersen, S. U. *Acta Chem. Scand.* **1997**, *51*, 135.

(42) A plot of $\Delta G^\ddagger$ versus ΔG° has a slope of $\alpha_G = 0.29$ ($r^2 = 0.991$). Although the plot is actually more parabolic ($r^2 = 0.994$), linearization does not affect the significance of the following. Plots of $\Delta H^\ddagger$ and $T\Delta S^\ddagger$ versus ΔG° lead to values of α_H and α_S of 0.53 ($r^2 = 0.991$) and 0.24 ($r^2 = 0.961$), respectively ($\alpha_G = \alpha_H - \alpha_S$). Although not discussed in detail in ref 41, very similar trends were observed in the reaction of *tert*-butyl bromide with some aromatic radical anions. In that case, values of α_G, α_H, and α_S of 0.38 ($r^2 = 0.976$), 0.51 ($r^2 = 0.955$), and 0.12 ($r^2 = 0.799$), respectively, can be derived from their reported data. It is striking that the enthalpic dependence is ca. 0.5 in both cases and that the apparent transfer coefficients (i.e., α_G) are determined by different entropic dependencies. It seems reasonable to expect that the overall entropy change in these reactions (i.e., $\Delta S^\circ_F + \Delta S^\circ_S$) is relatively independent of the mediator; therefore, $\Delta\Delta G^\circ \approx \Delta\Delta H^\circ$ and $\Delta\Delta H^\ddagger/\Delta\Delta H^\circ \approx 0.5$, as expected for any moderately driven activated process.

(43) Kojima, H.; Bard, A. J. *J. Am. Chem. Soc.* **1975**, *97*, 6317.

(44) Eberson, L. *Adv. Phys. Org. Chem.* **1982**, *18*, 79.

Table 4. Experimentally Determined Activation Parameters for the Reduction of DTBP by a Number of Aromatic Radical Anions

donor	log(*A*)	E_a (kcal mol^{-1})	log(k_{hom})[a] (M^{-1} s^{-1})	$\Delta S^{\ddagger}$[b] (cal mol^{-1} K^{-1})	$\Delta H^{\ddagger}$[c] (kcal mol^{-1})	$\Delta G^{\ddagger}$[a,d] (kcal mol^{-1})	α
chrysene	7.06	2.79	5.11	−21.2	2.49	8.81	0.226
isoquinoline	7.47	4.25	4.39	−19.3	3.95	9.72	0.271
pyrene	8.08	5.52	4.05	−16.5	5.22	10.15	0.297
anthracene	8.15	6.37	3.31	−16.2	6.07	10.91	0.319
9,10-diphenylanthracene	8.76	7.76	2.89	−13.4	7.48	11.47	0.346

[a] At 298 K. [b] From $\Delta S^{\ddagger} = R(\ln A - \ln Z - 0.5)$, $Z = 3 \times 10^{11}$ M^{-1} s^{-1}. [c] $\Delta H^{\ddagger} = E_a - 0.5RT$. [d] $\Delta G^{\ddagger} = \Delta H^{\ddagger} - T\Delta S^{\ddagger}$.

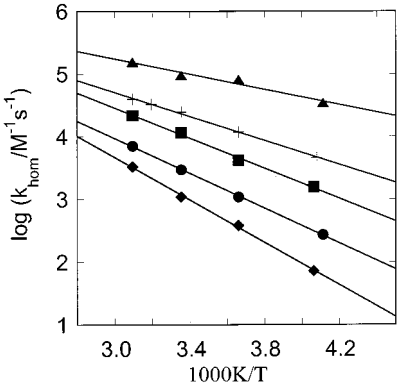

Figure 4. Arrhenius type plot showing the temperature dependence of the logarithm of the homogeneous ET rate constant log(k_{hom})$_{298}$ vs 1/*T* for the reaction of DTBP with the following homogeneous donors: (◆) diphenylanthracene, (●) anthracene, (■) pyrene, (+) isoquinoline, and (▲) chrysene.

relationship between the ionic radius (r_X) of singly charged anions and both the entropy in aqueous solution ($S°_{X-,aq}$) and the entropy change for the transfer of ions from water to DMF ($\Delta S°_{tr}$).[45] In this case the value of $S°_{t-BuO-,DMF}$ is determined from eq 24. We have assumed that ca. 60% of the surface of *tert*-butoxide is solvated as if it were hydroxide ion ($r_X = 140$ pm) while the hindered side, ca. 40% of the surface, is solvated as if it were an anion with $r_X = 210$ pm. This leads to values of $S°_{t-BuO-,aq}$ and $\Delta S°_{tr}$ of 16.8 and −24.2 cal mol^{-1} K^{-1}, respectively, giving $\Delta S°_S = -23.8$ cal mol^{-1} K^{-1}.

$$\Delta S°_S = (S°_{t-BuO-,DMF} - S°_{t-BuO\bullet,DMF}) - \Delta S°_{A\rightarrow A-,DMF} \quad (23)$$

$$S°_{t-BuO-,DMF} = S°_{t-BuO-,aq} + \Delta S°_{tr} = 43.1 \text{ cal mol}^{-1}\text{K}^{-1} \quad (24)$$

The predicted activation parameters are given in Table 5. Plots of the experimental and predicted rate constants as a function of the driving force derived from eqs 7−9 and the Eyring equation (log(Z) = 11.5) are shown in Figure 5. This figure shows the predicted rate constants calculated from the dissociative ET theory as derived originally by Savéant (eq 25)[6] and as originally reported by using the bond dissociation free energy (BDFE) rather than enthalpy[10] in the determination of the intrinsic barrier (eq 26; BDFE = 28.8 kcal mol^{-1}). For consistency, we have assumed that there is no contribution to the activation barrier from the avoided crossing energy (i.e., $H_{RP} = 0$), since neither of the previous models consider this factor.

$$\Delta G^{\ddagger} = \left(\frac{D+\lambda}{4}\right)\left(1 + \frac{\Delta G°}{D+\lambda}\right)^2 \quad (25)$$

$$\Delta G^{\ddagger} = \left(\frac{\text{BDFE}+\lambda}{4}\right)\left(1 + \frac{\Delta G°}{\text{BDFE}+\lambda}\right)^2 \quad (26)$$

A few observations are obvious from Tables 4 and 5 and Figure 5. About half of the discrepancy between the experimental and predicted data as originally reported in ref 10 may be attributed to the use of the BDFE rather than the BDE. At a glance, it appears that the incorporation of the cage and entropy effects accounts for the remainder of the difference.[46] While eqs 7−9 appear to correctly predict the activation free energy, some discrepancies remain. In particular, the predicted activation entropy is underestimated by a factor of 4, leading to an overestimate of the preexponential factor (log *A*) by about 2.5 orders of magnitude. This is compensated by an overestimate of the activation enthalpy. Furthermore, the model predicts an average α value of ca. 0.42 that is in the gray area between the concerted and stepwise mechanisms. The experimental value of ca. 0.3 is clearly consistent with the concerted mechanism. Finally, these models make no assumption concerning steric effects on the ET. Since we have shown that this effect accounts for a factor of about $10^{0.8}$, we should in principle increase the experimental log(k_{hom}) values by this amount in order to compare theory and experiment. This places the experimental points between the prediction based on the original Savéant theory and that from the latest revision including entropy effects.

The evidence above seems to indicate, as we originally suggested,[10] that nonadiabaticity effects may play a role in ET to dialkyl peroxides. This led us naturally to examine our experimental data on the basis of a theory for nonadiabatic dissociative ET recently published by German and Kuznetsov.[12] An ET reaction is viewed as nonadiabatic when the electronic coupling energy between the reactant and product states, H_{RP}, is distinctly below *RT*, i.e., 0.592 kcal mol^{-1} (200 cm^{-1}).[47] This is the equivalent to saying that the electronic transmission coefficient $\kappa_{el} \ll 1$ ($k = \kappa_{el} Z \exp[-\Delta G^{\ddagger}/(RT)]$) and that the reactant and product potential surfaces do not interact significantly. The calculation of H_{RP}, however, is rather complicated even for nondissociative type systems. For example, H_{RP} is often treated as an adjusting parameter to fit the experimental data with theoretical calculations. Because of this premise, the calculations to follow strictly allow a qualitative examination of our results in the framework of the theories of ET. Although the German and Kuznetsov (GK) theory has been developed to take into account quantum effects, for consistency with the

(45) A correlation between the crystallographic ionic radius, r_X, and the entropy in aqueous solution, $S°_{X-,aq}$, gives $S°_{X-,aq} = -250.2 + 1.91r_X$ ($r = 0.984$, eight ions. Marcus, Y. In *Ion Solvation*; Chichester; Wiley: Toronto, 1985.). A similar relationship is found for the entropy of transfer from water to DMF: $\Delta S°_{tr} = -53.9 - 0.28r_X$ ($r = 0.58$). The poor correlation coefficient for the second relationship is due to the dearth of data (only five ions) and the relative insensitivity of $\Delta S°_{tr}$ to the ionic radius (the range of values is from −87 meV/K for fluoride to −107 meV/K for thiocyanate).

(46) It should be noted that inclusion of the avoided crossing energy increases the predicted rate constant. For example, a value of $H_{RP} = 1.38$ kcal mol^{-1}, as used by Savéant in his treatment of *tert*-butyl bromide, increases the predicted rate constants by 1.5 orders of magnitude, so they appear to overlap the closed circles in Figure 2.

(47) Newton, M. D.; Sutin, N. *Annu. Rev. Phys. Chem.* **1984**, *35*, 437.

Table 5. Predicted Activation Parameters for the Homogeneous Reduction of DTBP by a Number of Aromatic Radical Anions

mediator ($E°$ vs SCE)	log(A)[a]	E_a (kcal mol^{-1})	log(k)[b] (M^{-1} s^{-1})	$\Delta S^{‡}$[c] (cal mol^{-1} K^{-1})	$\Delta H^{‡}$ (kcal mol^{-1})	$\Delta G^{‡}$[d] (kcal mol^{-1})	α
chrysene	10.68	7.17	5.42	−3.39	6.57	7.59	0.38
isoquinoline	10.60	8.49	4.39	−3.74	7.89	8.99	0.41
pyrene	10.56	9.27	3.76	−3.94	8.69	9.87	0.43
anthracene	10.52	10.01	3.19	−4.10	9.41	10.63	0.45
9,10-diphenylanthracene	10.48	10.91	2.48	−4.31	10.31	11.60	0.47

[a] Assuming log $Z = 11.5$. [b] 298 K. [c] Based on eq 8. [d] Based on eq 7.

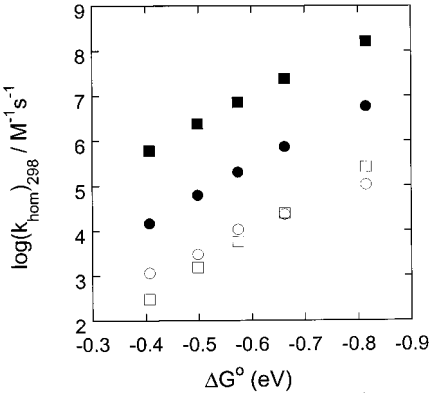

Figure 5. Plot of log(k)$_{298}$ vs driving force for the reaction of some aromatic radical anions with DTBP. The open circles are the experimental data. The open squares are derived using eqs 7−9. The closed circles and closed squares are derived from eqs 25 and 26, respectively.

Savéant adiabatic theory we considered the semiclassic limit of the nonadiabatic theory. In this limit, the harmonic approximation is used for the intramolecular vibrations and the solvent polarization, and the breaking bond is viewed as ruled by a Morse potential (eq 27), where r_0 is the equilibrium length of the breaking bond. In the analysis, an exponential is used for the repulsion potential for the product state (eq 28). A difference in this model compared with the Savéant model is that B and β_P can be different from BDE and β_R, respectively.

$$U_R = \mathrm{BDE}\{\exp[-2\beta_R(r - r_0)] - 2\exp[-\beta_R(r - r_0)]\} + \mathrm{BDE} \quad (27)$$

$$U_P = B\exp(-2\beta_P r) \quad (28)$$

In the GK theory the first-order rate constant for ET within the precursor complex, $k^{‡}$, has the form given in eq 29. Here, the two second derivatives of the functions f and g[48] are calculated at the saddle point, where the transfer coefficient α (eq 30, where $z = \exp[-\beta_R(r - r_0)]$ and $m = \beta_P/\beta_R$) and the bond length r are given by α‡ and $r^{‡}$, respectively.

$$k^{‡} = \frac{2\pi}{\hbar}(H_{RP})^2\left[\frac{|\mathrm{d}^2U_R/\mathrm{d}r^2|_{r_0}}{2\pi RT|\partial^2 g/\partial\alpha^2|_{\alpha_‡}|\partial^2 f/\partial r^2|_{r_‡}}\right]^{1/2} \exp[-\Delta G^{‡}/(RT)] \quad (29)$$

$$\alpha = \frac{1}{2}\left(1 + \frac{\Delta G°}{\lambda_s} + \frac{(B/\mathrm{BDE})z^{2m} - z^2 + 2z - 1}{\lambda_s/\mathrm{BDE}}\right) \quad (30)$$

The activation free energy $\Delta G^{‡}$ (eq 31) and the free energy $\Delta G°$ (eq 32) are functions of the bond elongation, $r^{‡} - r$, at the transition state (eq 31). Note that the $\Delta G°$ of eq 32 also equals $-F(E°_{\mathrm{ROOR/RO•,RO-}} - E°_{\mathrm{D/D•-}})$.

$$\Delta G^{‡} = (1 - z^{‡})^2\{\mathrm{BDE} + \lambda_s[1 - z^{‡} + (B/\mathrm{BDE})m(z^{‡})^{2m-1}]^{-2}\} \quad (31)$$

$$\Delta G° = \mathrm{BDE}(1 - z^{‡})^2 - Bz^{2m} - \lambda_s\frac{(B/\mathrm{BDE})m(z^{‡})^{2m-1} - 1 + z^{‡}}{(B/\mathrm{BDE})m(z^{‡})^{2m-1} + 1 - z^{‡}} \quad (32)$$

When the U_P is simply taken as the repulsive part of the Morse curve of the reagents,[6] i.e., for B/BDE $= \beta_P/\beta_R = 1$, eq 29 simplifies to eq 33, where $\Delta G^{‡}$ is as in eq 4. α (eq 30) then transforms into eq 10 (where $\Delta G° \equiv \Delta G°_C$).

$$k^{‡} = \frac{2\pi}{\hbar}(H_{RP})^2(16\pi RT\Delta G_0^{‡}\exp[-\beta_R(r^{‡} - r_0)])^{-1/2} \exp[-\Delta G^{‡}/(RT)] \quad (33)$$

The experimental second-order rate constant k_{hom} can be compared with the first-order rate constant $k^{‡}$ by taking into account the equilibrium constant for the diffusion-controlled formation of the caged donor−acceptor couple, K_d; therefore, $k_{hom} = K_d k^{‡}$. Since the acceptor is an uncharged species and thus no electric work is required to bring the donor D and the acceptor A together, K_d can be calculated by using the equation $K_d = [(4\pi Nr^r\delta r)/1000]$.[49] The ET rate, k_{hom}, is viewed as having no orientation preferences and occurring significantly only in a range of r values between r and $r + \delta r$. Assuming close contact of the ET couple, the separation distance r can be taken as $r_D + r_A$, i.e., the sum of the donor and acceptor radii. Reasonable values of δr appear to be ∼2 and ∼0.3 Å for adiabatic and nonadiabatic reactions, respectively.[49]

We started by carrying out a test calculation on the dissociative ET to *tert*-butyl bromide, already discussed as an adiabatic ET.[41,50] To compare reaction free energies similar to those used for the peroxides (see below), we focused on the data pertaining to two donors, the radical anions of quinoxaline ($E° = -1.64$ V, log $k_{hom} = 1.66$) and azobenzene ($E° = -1.32$ V, log $k_{hom} = -0.92$).[51] We used the following parameters: $E°_{t\text{-BuBr}} = -1.06$ V,[26] $r_D = 3.8$, effective $r_A = 2.8$ Å, $\beta = 1.43$ Å^{-1}, BDE = 66 kcal/mol,[50] B/BDE $= \beta_P/\beta_R = 1$, $\lambda_s = 15.1$ kcal/mol. The application of the GK approach led to the data reported in Table 6. It can be thus concluded that the ET to *t*-BuBr is indeed essentially adiabatic. Whereas the calculations were carried out for $\delta r = 0.3$ Å, it should be noted that using $\delta r = 2$ Å would have decreased H_{RP} by a factor $(0.3/2)^{1/2} = 0.39$. In addition, by using the experimental rate constants and the Eyring equation, κ_{el} can be evaluated to be ca. 1 (with $Z = 10^{12}$ M^{-1} s^{-1}), again pointing to an adiabatic dissociative ET.

(48) The two functions and their second derivatives are the following:[12] $f = (1 - \alpha)U_R(r) + \alpha U_P(r)$; $g = \alpha\Delta G° + \alpha(1 - \alpha)\lambda_s + (1 - \alpha)U_R(r^*) + \alpha U_P(r^*) - U_R(r_0)$; $\partial^2 f/\partial r^2 = 2(1 - \alpha)(2z^2 - z)\beta_R(\mathrm{BDE}) + \alpha(2\beta_P)^2 Bz^{2m}$; $\partial^2 g/\partial\alpha^2 = 2\lambda_s + [2\beta_R(\mathrm{BDE})(z - z^2) + 2\beta_P Bz^{2m}]\,(\mathrm{d}r/\mathrm{d}\alpha)$.

(49) Sutin, N. *Prog. Inorg. Chem.* **1983**, *30*, 441.
(50) Savéant, J.-M. *J. Am. Chem. Soc.* **1992**, *114*, 10595.
(51) Lund, T.; Lund, H. *Acta Chem. Scand.* **1986**, *B40*, 470.

Table 6. Nonadiabaticity Calculations for the Homogeneous Electron Transfer to DTBP, DCP, and *tert*-Butyl Bromide (*t*-BuBr)

acceptor	donor	ΔG^{o}[a,b] eV	log k_{hom} (DMF)	$r - r^*$ (Å)	α	H_{RP}[c,d] (cm^{-1})
DTBP	pyrene	−0.524	4.05	0.190	0.386	6.0−15.4
DTBP	fluoranthene	−0.249	2.15	0.230	0.445	5.8−15.1
DCP	9,10-diphenylanthracene	−0.517	4.40	0.186	0.383	6.2−16.1
DCP	naphthacene	−0.225	2.54	0.229	0.449	7.3−18.9
t-BuBr	quinoxaline	−0.580	1.66	0.378	0.418	82−212
t-BuBr	azobenzene	−0.260	−0.92	0.435	0.463	63−163

[a] $E^{\circ}_{DTBP} = -1.48$ V, $E^{\circ}_{DCP} = -1.32$ V. [b] $\lambda_{sDTBP} = 15.5$ kcal mol^{-1}, $\lambda_{sDCP} = 14.7$ kcal mol^{-1}. [c] B/BDE $= \beta_P/\beta_R = 1$. [d] Lower and upper values correspond to $\delta r = 2$ and 0.2 Å, respectively.

The calculations were carried out using data pertaining to the ET between either DTBP or DCP with donors selected to provide similar free energy values (Table 6). Besides the DTBP values given above, we used 2.9 Å and 14.7 kcal mol^{-1} for the effective radius and λ_s of DCP. β_R was calculated to be 2.56 and 2.97 $Å^{-1}$ for DTBP and DCP, respectively, through the O−O stretching frequency, ν_0,[52] and the relationship $\beta_R = \nu_0(2\pi^2\mu/\text{BDE})^{1/2}$, where μ is the reduced mass of the O−O atoms. The data reported in Table 6 show that for both peroxides and independently of the driving force, H_{RP} lies in the range 6−19 cm^{-1} and thus suggests nonadiabaticity in the ET. The effect of B/BDE was tested by using an arbitrarily selected value (0.5), taking into account that B is expected to be smaller than BDE.[53,54] In all cases, H_{RP} was found to decrease further by a factor of 15−20. Finally, by contrast with *t*-BuBr, κ_{el} was found to be significantly smaller than 1, namely, 0.01−0.02.

Finally, if one agrees that the actual preexponential factor Z is 2 orders of magnitude lower than the adiabatic limit, then the activation entropies reported in Table 4 should be adjusted from a range −21 to −13 cal mol^{-1} K^{-1} to a range −11 to −3 cal mol^{-1} K^{-1}. Of course, the activation ethalpies are not affected. This reduces the activation free energies to a range 5.5−8.1 kcal mol^{-1}. This points to the pitfall in converting the Arrhenius preexponential factor (log A) into an activation entropy, since in the absence of clear evidence the choice of log Z may be arbitrary.

Summary and Conclusions

A clearer picture now emerges of the dynamics of the concerted dissociative reduction of peroxides. In our original communication we suggested that the discrepancy between the experimentally determined rate constants and the Savéant theory was about 4 orders of magnitude, about half of which could be attributed to a distance dependence on the ET caused by a steric effect. The other half was attributed to an intrinsic nonadiabatic effect.[10] However, in our original report the BDFE and not the BDE was used in the estimate of the intrinsic barrier. The use of the BDE[11] lowers the theoretical estimate by about 1.5 orders of magnitude, leaving the discrepancy between theory and experiment as 2−2.5 orders of magnitude. The effect of steric hindrance, estimated by comparison of the reduction of DTBP with DNBP, was found to account for a factor of 6, still leaving a discrepancy of 1.2−1.7 order of magnitude. The temperature dependence of the reduction of DTBP leads to low preexponential factors. These unusually low preexponential factors are not predicted by the Savéant theory even after accounting for cage and entropy effects.[11] Although the free energy dependence is not easily explained, their unusually low values are consistent with a nonadiabatic effect. On the other hand, GK theory predicts the low preexponential factors found for DTBP because of a weak electronic coupling ($H_{RP} \approx 15$ cm^{-1}). Thus, we conclude that the concerted dissociative reduction of the peroxides is nonadiabatic.

With this conclusion it is interesting to speculate why the reduction of DTBP is nonadiabatic while the reduction of *tert*-butyl bromide is apparently adiabatic. The stretching of the C−Br bond results in a change in the dipole moment of the bond because of electron redistribution. The bromine atom that will eventually accept an electron becomes more electron-deficient as the bond lengthens. This seems ideal for the concerted dissociative reduction, since the molecular trajectory along the reaction coordinate sets up the Br group to accept an electron. On the other hand, the peroxides are completely symmetrical, so while the stretching of the O−O bond may lead to a change in polarizability of the bond, there is no change in dipole moment. At the transition state it is not clear to which fragment the electron will go; somehow the symmetry must be broken. Under these conditions, perhaps it is not surprising that there is poor electronic coupling between the reactant and the product surfaces.

Acknowledgment. We dedicated this to Dr. Keith Ingold on his 70th birthday and in recognition of his outstanding contributions to science. We thank Professor J.-M. Savéant for helpful comments. M.S.W. thanks the Natural Sciences and Engineering Research Council of Canada and the University of Western Ontario (ADF) for funding. F.M. thanks the Consiglio Nazionale delle Ricerche for financial support (Short-term Mobility Program).

JA9906148

(52) Lin-Vien, D.; Colthup, N. B.; Fateley, W. G.; Grasselli, J. G. *The Handbook of Infrared and Raman Characteristic Frequencies of Organic Molecules*; Academic Press: Toronto, 1991.

(53) Marcus, R. A. *Acta Chem. Scand.* **1998**, *52*, 858.

(54) Daasbjerg, K.; Jensen, H.; Benassi, R.; Taddei, F.; Antonello, S.; Gennaro, A.; Maran, F. *J. Am. Chem. Soc.* **1999**, *121*, 1750.